Microstructures and Strengths of Metals and Ceramics made by Photopolymer-based Rapid Prototyping

Walter Zimbeck, Matthew Pope, Ceramic Composites, Inc., Annapolis, MD 21401 410-224-3710; and R.W. Rice, Consultant, Alexandria, VA 22301 703-971-4379

ABSTRACT

Metal and ceramic flexure specimens were fabricated using a photopolymer-based rapid prototyping technique. Photosensitive resins (inks) were produced by dispersing 50 - 55 vol% metal or ceramic powders in a photopolymer resin. Laminates 0.2" thick were built up by repeated application of layers 3 - 10 mils thick followed by curing under a UV flood lamp with photomasks. The layered samples were thermally processed to remove the photopolymer binder and sintered to high density. Densities, microstructural characterization and flexure strengths are reported for silicon nitride, alumina, zirconia, stainless steel, and tungsten.

I. INTRODUCTION

Freeform fabrication of metal and ceramic components offers a number of advantages including cost and time efficient functional prototyping and small lot production, the ability to fabricate complex shaped designs using materials which have historically been difficult to shape form, and the possibility of fabricating new material architectures with unique properties tailored for specific applications. In demonstrating the feasibility of freeform fabrication processes, several issues must be addressed:

1. Demonstration that desired physical properties are achievable;
2. Determination of dimensional accuracy and uniformity; and
3. Demonstration of shape intricacy capability.

This paper reports on progress made by Ceramic Composites, Inc. (CCI) on demonstrating the physical properties achievable by photopolymer-based fabrication of a variety of metals and ceramics. Photopolymer-based freeform fabrication of metals and ceramics has several unique and significant advantages relative to other SFF processes such as LOM of ceramic and metal tapes, Fused Deposition of Ceramics, Selective Laser Sintering and 3D Printing. These advantages are based in the large existing infrastructures of core related technologies. For example, 1) the photopolymer industry is large and growing with a wide variety of existing resins and a strong R&D infrastructure for new resin development; 2) the photolithography infrastructure supporting the electronics industry is substantial and provides the hardware base for large area, high speed and high accuracy photocuring; and 3) photopolymer-based fabricators, led by 3D Systems' SLAs are by far the most prevalent fabricators in use and come with a considerable body of R&D from which new innovations and process improvements will emerge.

W.R. Grace and Co. initiated development of ceramic/photopolymer resins in 1992, however due to major corporate restructuring, Grace abandoned development and the technology was transferred to CCI in 1994. CCI seeks to commercialize this technology through the sale of metal and ceramic resins compatible with current photopolymer-based fabricators and/or by offering service bureau capability for metal and ceramic components.

Photopolymer-based fabrication of metal and ceramic objects entails formulating a colloidal suspension of fine inorganic particles in a photosensitive resin. This metal or ceramic resin can be used as the feedstock material in photopolymer-based fabricators such as 3D Systems' SLA machines and Cubital's Solider systems to build "green state" metal or ceramic objects. Subsequent thermal processing of the part burns-off the photopolymer binder and sinters the inorganic particles to high density.

Photopolymer-based fabrication of metals and ceramics poses a number of challenges which are not encountered with conventional StereoLithography and Solid Ground Curing of polymer parts. The initial challenges are:

- Achieving high solids loading in the resins while maintaining low viscosity and stable particle suspension;
- Formulating the resin to provide good interlayer adhesion, minimal shrinkage during cure, and nondisruptive binder burnout;
- Determining the binder burnout and densification conditions to give high density and desirable properties;

The remainder of the paper describes how these issues were addressed and presents results for the various materials under development.

II. EXPERIMENTAL

II.1 Resin Formulation

A number of tradeoffs must be made in formulating metal or ceramic resins. For high density and high strength parts it is desirable to maximize the solids volume fraction of fine sinterable particles in the resin. For materials with high specific gravity, such as tungsten (19.3 g/cc), smaller particle size powders are additionally appealing because of their lower sedimentation rates (Stoke's Law), thereby enabling stable suspensions. However, smaller particles and higher solids loading result in higher viscosity and commensurately longer layer application times. To achieve as-sintered material with high density (>95%), 45 vol% solids loading in the resin is typically a minimum requirement, with >50 vol% desired. In order to achieve high solids loadings with fine particles, resin formulations must typically include dispersants and/or coupling agents for steric and electrostatic stabilization to prevent particle agglomeration. Smaller particles and higher solids loadings also result in lower cure depth, which require the use of thinner layers.

Typically a blend of at least two photomonomers is used in order to achieve the desired resin properties. Key resin properties are:

- low viscosity
- stable particle suspension
- cured surface tack for interlayer adhesion
- low cure shrinkage
- sufficient cured strength, rigidity and toughness

In addition to dispersants and/or coupling agents, other additives are commonly used such as plasticizers, thickeners, solvents, and anti-foaming agents to improve these and other resin properties. The procedure used to mix the ceramic or metal resins entails mixing the liquid ingredients together followed by addition of the ceramic or metal powders. Typically, the powders are added in increments to maintain flowability of the resin.

The final addition to the mixture are the photoinitiators or sensitizers. The photoinitiators act as absorption sites for the incident photons producing free radicals which initiate crosslinking of the monomers. Photoinitiators are typically added in concentrations of 0.1 - 4 % based on the weight of the crosslinkable monomers. The type and concentration of photoinitiators used has a significant effect on cure depth, speed of cure and the working curve of the resin.[1]

II.2 Layer Application and Curing

For the purposes of building flat samples, a manual laminate building apparatus is used (Figure 1). The piston height is set to a depth below the top surface equal to the desired layer thickness. Ceramic or metal resin is poured onto the piston and a blade caster resting on the top surface is used to spread a uniformly thick layer of resin. The layer is cured using an ultraviolet lamp (Fusion UV Curing Systems) and a photomask, which is placed just above the surface of the resin. By repeating the process, multilayer laminates are built.

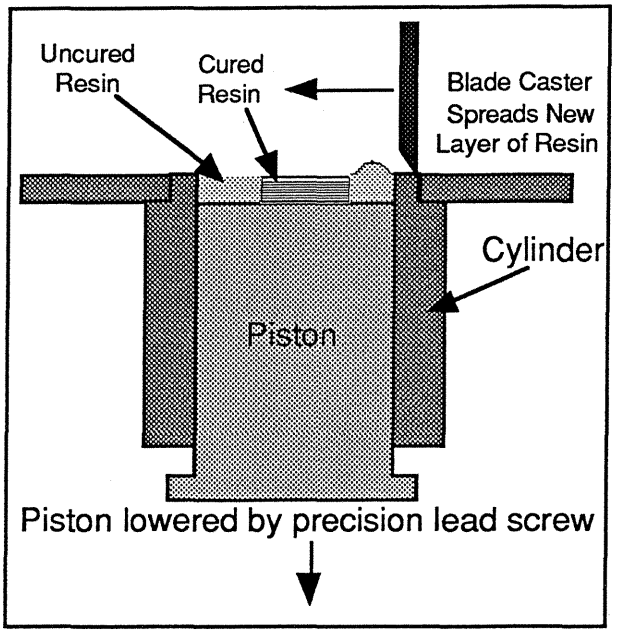

Figure 1. Laminate building apparatus

II.3 Binder Removal and Sintering

Once the green state part is built, it is thermally processed to remove the organic (mostly photopolymer) binders and subsequently sintered to high density. The binder burnout stage is critical and requires carefully controlled temperature ramp-up, particularly when the organic constituents begin to decompose and gaseous by-products are generated. Gases formed during rapid decomposition can build up internal pressure and cause delamination, blistering and bloating of the part, especially in thick sections. Differential scanning calorimetry (DSC) and thermo-gravimetric analysis (TGA) can be used to determine the temperatures at which decomposition occurs. A burnout schedule can be derived from these data which results in non-disruptive rate of weight loss during the heating cycle. Above 500°C, most of the organic phases have been removed and heating can be continued up to the respective sintering temperatures. Sintering schedules commonly used in powder metallurgy or powder processing of ceramics can be used to sinter components to high density providing sufficient green densities had been achieved.

III. RESULTS

III.1 Alumina

Alumina resins were made using A16 SG powder (~0.4 μm average particle size, APS) from Alcoa. The photopolymer formulation consisted of three commercially available acrylate based monomers. At 45 vol% solids loading the resin viscosity is ~1200 cPs. At 50 vol% solids the viscosity increases to ~3,000 cPs, still well within the practical viscosity range for layer

building using the blade casting technique shown in Figure 1. Crystalline alumina shows high spectral transmittance (~0.8) from 300 nm out to about 4 μm wavelengths,[2] and the alumina resins show good depth of penetration at the principal output wavelengths of the lamp (400 - 425 nm). At a five second exposure, which roughly correlates to an exposure dose of 100 mJ/cm^2, the cure depth is 0.033". At two and one second exposures the cure depths are 0.015" and 0.003", respectively.

Using a 50 vol% alumina resin, samples 0.1" and 0.2" thick were built with 0.005" thick layers. Some delamination problems were encountered when layers 10 and 15 mils thick were used, possibly due to stresses resulting from shrinkage of the resin during curing. Differential scanning calorimetry (DSC) and thermogravimetric analysis (TGA) tests were performed on small pieces of cured alumina resin. TGA tests showed weight loss beginning at ~150°C and ending at ~480°C. DSC tests showed two exothermic peaks in this range, one centered at ~275°C and one centered at ~400°C. Based on this data an 18 hour binder burnout cycle was derived. Sample weight loss during binder removal is in the range 15 - 18%. After binder removal, the samples were sintered in air at 1600°C for 2 hours.

Sintered densities ranged from 90% to greater than 98% theoretical. Samples with densities below 98% exhibited voids caused by air bubbles in the resin and delamination defects particularly near the edges. Samples with densities exceeding 98% showed no voids or delaminations and were the result of improved resin preparation and layer building techniques. Figure 2 shows opposing fracture surfaces of an alumina sample with a large void at the corner and two delaminations. Figure 3 shows a dense alumina sample with no laminar artifacts visible which was produced further into the development. The sintered grain size of these samples was typically in the range 30 to 50 microns, indicating extensive grain growth due to over sintering.

Strength data was obtained by three point flexure tests. Small flexure samples were diced from the larger specimens and tested as-is without surface grinding or chamfering. Samples with density >98% (see Figure 3) exhibited strengths of ~350 MPa (53,700 psi) which is typical of cold pressed and sintered A16 alumina. Samples with delaminations and voids (see Figure 2) exhibited strengths in the range 200 - 300 MPa.

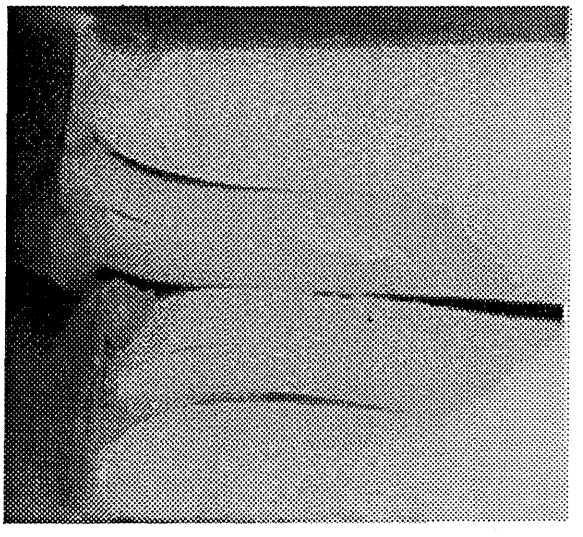

Figure 2. Alumina sample fracture surface showing delamination and void.

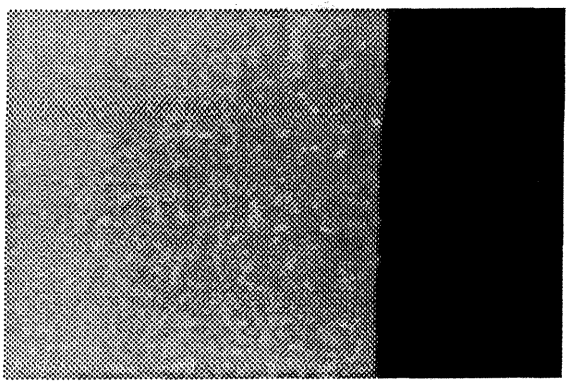

Figure 3. Alumina sample fracture surface showing no lamination artifacts or visible defects.

III.2 Silicon Nitride

Silicon nitride resins were made with a 70:30 mixture of SN E3 (0.7 μm APS) and SN E10 (0.3 μm APS) powder from Ube. Alumina and yttria sintering aids were used at 5 wt% of the silicon nitride powder. The photopolymer mixture that was used for alumina resins was also used for the silicon nitride resins. At 45 vol% solids the silicon nitride resin has a viscosity of ~3,500 cPs and at 50 vol% the viscosity increases to ~5,000 cPs. Relative to the alumina resins, the silicon nitride resins exhibit very limited cure depth. The maximum cure depth observed was 0.004". Griffith and Halloran[3] have derived a relationship between cure depth and resin properties which shows that the penetration depth is inversely proportional to the square of the difference in refractive index (RI) between the ceramic and the UV curable solution ($1/\Delta n^2$). The RI of the photopolymer mixture is roughly 1.45. The RI of alumina is 1.7 and the RI of silicon nitride is 2.1. Thus, the $1/\Delta n^2$ factor is roughly 7 times higher for alumina resins compared to silicon nitride resins, accounting for much of the observed difference in cure depth.

Using a 50 vol% silicon nitride resin, samples 0.1" thick were built using a layer thickness of 0.002". A few samples were made with 0.005" thick layers, resulting in uncured resin between each cured layer. The uncured resin layers act as slip planes which accommodate shrinkage during cure so that no curling of these samples was observed. However, binder burnout and sintering of these samples resulted in severe delaminations. A binder burnout schedule identical to the one used for alumina resins was used for the silicon nitride samples.

Several different sintering schedules were carried out under 1 atm. nitrogen, but difficulties in temperature control resulted in samples that were at best 90% dense with some degree of delamination. The maximum three point flexure strength of these samples was 412 MPa and the laminar nature was evident in the fracture surfaces. One silicon nitride sample was hot pressed at 1800°C. This sample was fully dense with no laminar defects visible and flexure strengths ranging from 505 to 757 MPa with an average from three specimens of 636 MPa. Figure 4 is an SEM photograph of the microstructure of the hot pressed silicon nitride sample showing a high concentration of the acicular β grains.

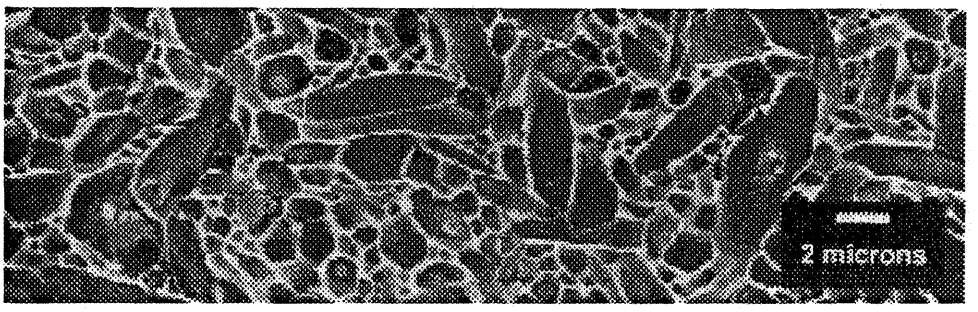

Figure 4. 5000x electron micrograph of the hot pressed silicon nitride sample.

III.3 Stainless Steel

Stainless steel resins were made using 316L stainless steel powder with particle size <16μm (Anval, Inc.). The resin formulation had to be adjusted to include higher viscosity monomers which prevented rapid settling of the relatively large and dense (ρ = 7.9 g/cc) stainless steel particles. Resins with 55 vol% solids content exhibited relatively low viscosity. The viscosity of these resins was not measured, although they have lower viscosity than the 45 vol% alumina resins, which were measured at 1,200 cPs. Stainless steel is opaque at the wavelengths of interest; thus, light penetration is dependent on spacing between particles and reflectivity of the particles. At 400 nm, roughened stainless steel plate has a reflectivity of ~0.9[4]. The reflectivity would likely be lower for -16 μm stainless steel particles. The maximum cure depth achievable with the 316L resins was 0.003" - 0.004" with exposure doses comparable to those used for the silicon nitride resins.

Using a 55 vol% 316L resin, samples 0.1" and 0.2" thick were built with 0.002" thick layers. Binder removal and sintering of the stainless steel samples was conducted in a reforming gas environment (4% H_2 in argon) to prevent oxidation of the stainless steel. In this atmosphere, the onset of thermal degradation begins at ~280°C and continues up to ~480°C. In this temperature range, the ramp rate was held to 0.3°C/minute. Three sintering temperatures were evaluated, 1000°C, 1100°C and 1125°C, which resulted in sample densities of 81%, 92% and 95%, respectively. The samples sintered at 1100°C were placed on graphite setter material during sintering. These samples exhibited brittle fracture behavior and strengths between 314 and 355 MPa. The samples sintered at 1125°C were placed on alumina setter material during sintering and showed considerable ductility in fracture and strengths between 397 and 455 MPa. The brittle behavior of the samples sintered on graphite setter material was probably a result of carbide formation on the surface in contact with the graphite. The ductile nature of the other stainless steel samples indicates that if any carbon residue is left during binder burnout, it is not significant enough to cause carbide embrittlement of the stainless steel. Figure 5 is a photograph of one of the 95% dense 316L samples after flexure testing showing the ductility of the material. Figure 6 shows a fracture surface of another 95% dense 316L sample. The 0.002" thick layers are barely visible in this photograph, although the laminar artifacts did not appear to weaken the material and may tend to strengthen the material by redirecting crack growth along the interface between layers.

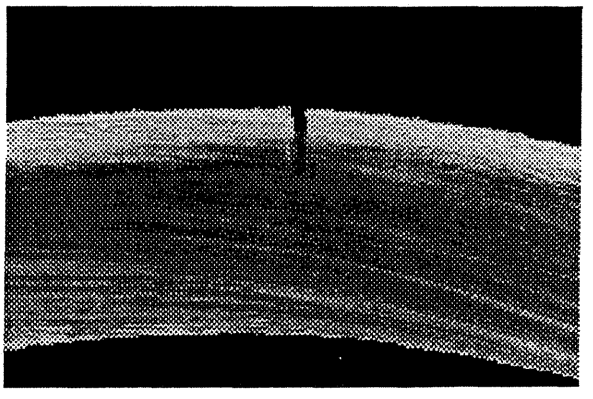

Figure 4. 316L stainless steel sample after flexure test, showing considerable ductility.

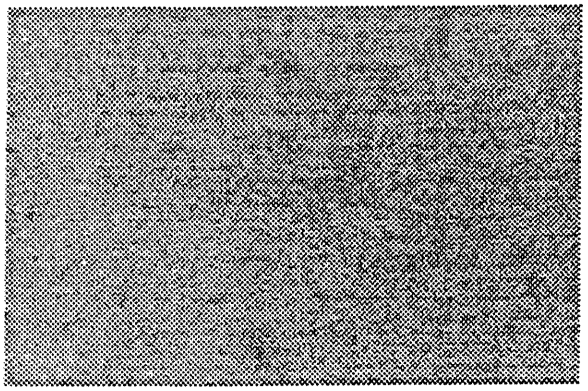

Figure 5. Fracture surface of a 316L stainless steel sample showing 0.002" thick layers.

III.4 Tungsten

Tungsten's high density (19.3 g/cc) requires that special consideration be given to resin formulation in order to minimize particle settling rates. High settling rates will result in non uniform intra- and inter-layer solids volume fraction and non uniform shrinkage during sintering. High viscosity monomers and additives are being used to reduce particle settling in the resins. Stokes' Law shows that particle size also has a large effect on settling rates. While smaller particles result in lower settling rates, other effects must also be considered and tradeoffs made. For example, smaller particles are desirable for better sinterability, fine sintered grain size and generally higher strength as well as lower settling rates in the resin. However, smaller particles result in higher resin viscosity at the same solids volume fraction or lower solids volume fraction at the same resin viscosity. As shown by Griffith and Halloran (see reference 3), smaller particle size also results in shallower cure depth. Thus, resins were formulated with particle size powders ranging from 0.8 μm up to 10 μm APS and settling rates, viscosity and cured depth tests were conducted. Although testing is not complete, results indicate that particles sizes between 2 and 5 μm are a good compromise, providing satisfactory cure depth (0.002" - 0.003"), workable settling rates, and solids loadings of 50 vol% while maintaining practical viscosity.

The 0.002" - 0.003" cure depths achievable with these tungsten resins require an exposure dose of roughly 3,000 mJ/cm^2, which is 2 - 3 times higher than used on the stainless steel resins. One factor which may at least partially explain the higher required dose, is tungsten's relatively high absorptivity at the wavelengths of interest.[5] The much higher absorptance of tungsten at 400 nm (~0.52) compared to stainless steel (~0.12) indicates that the tungsten particles act as absorption sites and are competing with the photoinitiators for incident radiation. Thus, higher exposure doses are required to achieve curing of the tungsten resins.

IV. SUMMARY AND CONCLUSIONS

The objective of this work was to demonstrate that physical properties, particularly strength, similar to conventionally processed materials could be achieved by photopolymer-based freeform fabrication. A variety of metal and ceramic resins were formulated and samples were built using a manual laminate building apparatus and a UV flood lamp/photomask system. Density and flexure strength data showed that high densities and strengths could be achieved using this process. Resin properties and as-sintered densities and strengths of all the materials are summarized in Table 1.

Potential limitations to using these resins with commercial photopolymer-based fabricators were also identified. Based on the resin properties observed, it appears that alumina resins have high compatibility with commercial photopolymer-based fabrication systems. Work is underway

with alumina resins to demonstrate this compatibility and complex shape building capability. Similar compatibility is expected for other oxide ceramics such as silica, zirconia, mullite, etc. The compatibility of silicon nitride and stainless steel resins with commercial systems is lower primarily due to the limited cure depth (0.003" - 0.004" maximum) of these resins. This is at the typical lower limit of layer thicknesses currently recommended with commercial systems, although alternative layer application methods which can apply thinner layers uniformly could potentially be developed for these commercial systems. Tungsten resins have limited cure depth (0.002" - 0.003" maximum) but also involve challenges not encountered with the other materials. Keeping the tungsten particles suspended in the resin is difficult and may require a layer application system which includes an agitated resin storage tank to maintain suspension. Tungsten resins also appear to have much higher E_{crit}, the minimum exposure dose required to achieve gelation, which could significantly extend build times. Further research will more clearly define the limitations and equipment requirements for tungsten resins.

Table 1. Summary of resin properties and as-sintered densities and strengths.

Material	Solids vol% in Resin	Resin Viscosity	Cure Depth (max)	Density	Flexure Strength (max)
Alumina	50	~3000 cPs	>0.033"	>99%	360 MPa
Zirconia*	40	---	~0.006"	>97%	530 MPa
Si_3N_4	50	~5000 cPs	0.004"	90% & >99%#	412 & 757# MPa
Stainless Steel	55	<1200 cPs	0.003"	95%	455 MPa
Tungsten	50	----	0.0025"	----	-----

*Zirconia resin developed and tested at W.R. Grace prior to CCI involvement.
#This silicon nitride sample hot pressed to full density.

V. ACKNOWLEDGMENTS

Ceramic Composites, Inc. would like to thank the NASA and Air Force SBIR programs for supporting this work.

VI. REFERENCES

[1]Jacobs, P.F., "Rapid Prototyping and Manufacturing, Fundamentals of StereoLithography," Society of Manufacturing Engineers, Dearborn, MI, 1992, pp. 87 - 91.
[2]Thermal Radiative Properties of Non Metallic Solids, Vol 8, Y.S. Touloukian and B.P. DeWitt, Thermophysical Properties Research Center, Purdue University, ISI/Plenum, 1970, pp. 168 - 169.
[3]M.L. Griffith, and J.W. Halloran, *Proceedings of the SFF Symposium*, University of Texas at Austin, Austin Texas, 1994, pp. 396 - 403.
[4]Themal Radiative Properties of Metallic Elements and Alloys, Vol 7, Y.S. Touloukian, and B.P. DeWitt, Thermophysical Properties Research Center, Purdue University, ISI/Plenum, 1970, pp. 1293 - 1294.
[5]Themal Radiative Properties of Metallic Elements and Alloys, Vol 7, Y.S. Touloukian, and B.P. DeWitt, Thermophysical Properties Research Center, Purdue University, ISI/Plenum, 1970, pp. 825 - 826 and 1293 - 1294.